

See discussions, stats, and author profiles for this publication at: <https://www.researchgate.net/publication/280042222>

Feasibility Study Of Gnss As Navigation System To Reach The Moon

Article in *Acta Astronautica* · July 2015

DOI: 10.1016/j.actaastro.2015.06.007

CITATIONS
54

READS
1,867

6 authors, including:



Vincenzo Capuano
California Institute of Technology

35 PUBLICATIONS 416 CITATIONS

[SEE PROFILE](#)



Jérôme Leclère
MacDonald, Dettwiler and Associates Ltd

35 PUBLICATIONS 423 CITATIONS

[SEE PROFILE](#)



Pierre-André Farine
École Polytechnique Fédérale de Lausanne

207 PUBLICATIONS 1,693 CITATIONS

[SEE PROFILE](#)

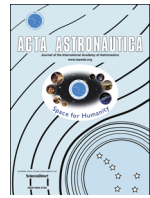
Some of the authors of this publication are also working on these related projects:



Cubesat ADCS subsystem [View project](#)



SANAG (Spaceborne Autonomous Navigation based on GNSS) [View project](#)



Feasibility study of GNSS as navigation system to reach the Moon[☆]



Vincenzo Capuano, Cyril Botteron, Jérôme Leclère, Jia Tian, Yanguang Wang,
Pierre-André Farine

École Polytechnique Fédérale de Lausanne (EPFL), Switzerland

ARTICLE INFO

Article history:

Received 20 November 2014
Received in revised form
31 March 2015
Accepted 6 June 2015
Available online 6 July 2015

Keywords:

Space navigation
GNSS
GPS
GNSS receiver
Moon Transfer Orbit (MTO)
Moon exploration

ABSTRACT

Reaching the Moon poses very strict requirements in terms of performance, flexibility and cost for all the spacecraft subsystems. These requirements become more stringent if the mission is designed to be accomplished using a small spacecraft. The navigation subsystem is without any doubts essential and nowadays, several systems offer different solutions to the navigation problem. Global Navigation Satellite Systems (GNSSs) such as GPS, GLONASS, or the future Galileo and BeiDou systems, introduce an easier way to provide an autonomous on-board orbit determination system; they only require an on-board GNSS receiver, with low-cost, low-power consumption and limited mass and volume. While GNSS receivers have been already exploited with success for Low Earth Orbit (LEO), their use for very High Earth Orbit (HEO) up to the Moon altitude is still at the research stage. In this context, the purpose of the present work is to determine the potential achievable accuracy of a code-based GNSS receiver solution, during the whole trajectory to reach the Moon. GPS, Galileo, and GPS-Galileo combined (dual constellation) solutions are estimated, by considering constellations availability, pseudorange error factors and geometry factors. Unlike previous investigations, our study is making use of the very accurate multi-GNSS constellation simulator "Spirent GSS8000", which supports simultaneously the GPS and Galileo systems with L1, L5, E1, and E5 frequency bands. The contribution of this study, clearly demonstrates that GNSS signals can be tracked up to the Moon's surface, but not with the current GNSS receiver's technology for terrestrial use. We consider and discuss a possible navigation solution that uses a double constellation GPS-Galileo receiver aided by an on board orbital filter system in order to improve the accuracy of the navigation solution and achieve the required sensitivity.

© 2015 IAA. Published by Elsevier Ltd. All rights reserved.

1. Introduction

In the last few years, GNSSs originally designed to provide position, velocity and timing (PVT) services for

land, maritime, and air users, have been adopted for a wide range of other applications also in Low Earth Orbit (LEO), such as for real-time navigation, formation flying, remote sensing of the Earth, precise time synchronization, orbit determination and atmospheric profiling. In fact, a GNSS receiver can maximise the autonomy of a spacecraft and reduce the burden and costs of network operations. For these reasons, the GNSS-use is attractive also for applications at higher Earth orbit; such as for Medium Earth Orbit (MEO), Geostationary Orbit (GEO), High Earth

[☆] This paper was presented during the 65th IAC in Toronto.

E-mail addresses: vincenzo.capuano@epfl.ch (V. Capuano), cyril.botteron@epfl.ch (C. Botteron), jerome.leclere@epfl.ch (J. Leclère), jia.tian@epfl.ch (J. Tian), yanguang.wang@epfl.ch (Y. Wang), pierre-andre.farine@epfl.ch (P.-A. Farine).

Orbit, and Highly Elliptical Orbit (HEO) missions, including Moon Transfer Orbits (MTO). However, space represents a challenging operational environment, where the GNSS receiver performance is considerably affected. The receiver performance is in fact strongly influenced by high space-craft translational and rotational dynamics, weaker received signals power, thermo-mechanical stresses and possible multipath effects, self-induced from the nearby surfaces or due to reflection with other vehicles. Moreover, the GNSS satellites geometry at high altitude, depending on the receiver sensitivity, can drastically reduce the navigation solution accuracy, due to the very limited region in the field of view where the GNSS satellites can be observed.

Part of our study about the GNSSs received signal characteristics in MEO, GEO and HEO has already been presented in [1]. Other similar investigations for the case of GEO and HEO have been done in [2–7]. Ref. [2] presents initial simulation results obtained in GEO from tests of the *PiVoT* GPS receiver tracking developed at *NASA Goddard Space Flight Center* (GSFC) and describes the capability that has to be added to operate in HEOs. The autonomous tracking of GPS signals within a HEO has been demonstrated for the first time on board the *AMSAT-OSCAR 40* spacecraft flying in a 1000 by 59,000 km altitude orbit as described in [3,4] where encouraging experimental results are reported. Several aspects of the GNSS use in LEO, GEO, HEO and beyond have been discussed and analysed in [5]. Results of additional hardware in-the-loop tests that assess the performance of a GPS receiver developed by GSFC in various HEOs are reported in [6]. Ref. [7] shows by means of simulations that using GNSS for GEO/GTO is feasible, even considering current spaceborne receivers state-of-the-art.

This paper instead, as done in [8–10] aims to investigate the use of a GNSS receiver for the specific case of MTO. More specifically, while [8] assesses the performance of a developed receiver (the *Navigator* GPS receiver made by GSFC) in three small representative segments of a manned lunar mission trajectory, more similarly to [9,10] this paper presents a feasibility study of the GNSSs as navigation system to reach the Moon. However, unlike [9,10], our study aims to estimate the GNSS availability and the consequent positioning accuracy achievable more in details for different combinations of receiver sensitivities and signals, of more than one constellation.

In this paper, different values of receiver sensitivity (-159 , -164 and -169 dBm) are considered according to the received power at the receiver during the full trajectory to the Moon, in case of use of GPS, Galileo, and GPS-Galileo combined (double constellation). Furthermore a theoretical study based on well-known models proves that such sensitivity values are achievable in acquisition and tracking. The signals considered are GPS L1 C/A, GPS L5, Galileo E1 and Galileo E5. Then, the GNSS performances are evaluated in terms of availability, pseudorange error factors and geometry factors, for a HEO with perigee in LEO and apogee at Moon altitude. Our analysis is carried out by using our multi-GNSS constellation simulator “Spirent GSS8000”, which supports simultaneously the GPS and Galileo systems with L1, L5, E1, and E5 frequency bands.

The rest of the paper is organised as follows. Section 2 presents the simulation models and the assumptions we used for our analysis, while Section 3 reports the signals performances obtained as simulations result. The minimum required sensitivity values are then defined in Section 4, where a theoretical analysis demonstrates they can be achieved in the acquisition and tracking processes. Sections 5 and 6 respectively outline the consequent signals availability and the expected navigation performance. In particular pseudorange errors and Geometry Dilution of Precision (GDOP) are evaluated and the achievable performance using an orbital filter is then briefly discussed.

2. Simulation models and assumptions

2.1. Constellations model assumptions

According to [11], we assumed a GPS constellation consisting of a nominal 24 operational GPS satellites allocated in six orbital planes (such assumption is conservative since there are generally more satellites operational than the nominal 24 GPS [12]), and as defined in [13] a Galileo constellation including 27 satellites, allocated in 3 orbital planes.

2.2. Signals model assumptions

In order to simulate realistic GNSS signals at very high altitudes, the GNSS transmitter models and signal strength offsets must be selected carefully. We consider the GPS L1 C/A signal and only the pilot channels of GPS L5, Galileo E1, and Galileo E5a+E5b (the sum of the two signals Galileo E5a and Galileo E5b) signals, because as described in Section 4.1 the pilot signals allow a longer coherent integration time.

The Spirent simulator has the capability to generate GNSS signals whose corresponding signal strength is modelled to provide realistic signal levels at the receiver position by modelling the gain patterns of both transmitter and receiver antennas and taking into account the free space signal propagation losses. Each satellite signal strength at the receiver position P_r is modelled as [14]

$$P_r = P_{ICD} + O_G + 20 \times \log_{10}(R_0/R) - L_{TX} - L_{RX \text{ (dBm)}} \quad (1)$$

where

P_{ICD} is the guaranteed minimum signal level for the GNSS signals on the Earth, as provided in the SIS ICDs. O_G “Global Offset”. This value is chosen to match the performance obtained when using the simulator with the performance obtained when real signals are received.

R_0 is the reference range used for inverse-square variation calculation and equal to the range from a receiver to the GNSS satellite at zero elevation.

$$R_0 = \sqrt{(\text{satellite orbit radius})^2 - (\text{earth radius})^2}$$

R is the range from GNSS satellite to the receiver.

L_{TX} is the gain/loss from the GNSS satellite transmit antenna in the direction of the receiver that takes into

account the radiation pattern of the antenna.

L_{RX} is the gain/loss from the receiver antenna in the direction of the GNSS satellite, which in our paper has been considered as constant.

For the considered signals GPS L1 C/A, GPS L5Q, Galileo E1c and Galileo E5aQ+E5bQ, **Table 1** reports the guaranteed minimum received signal power on the Earth P_{ICD} , according to [13–16]. **Table 1** also reports a global signal strength offset O_G used in Spirent for our simulations. This global signal strength offset takes into account for the difference between the guaranteed minimum signal level and the expected real one. Indeed, typically the transmitted signal powers are from 1 to 5 dB higher than the minimum received signal power value [12], therefore a middle value of 3 dB has been chosen. The 12 channels of the Spirent simulator GPS unit and the other 12 of the Galileo unit were configured to simulate respectively the strongest 12 GPS signals and the strongest 12 Galileo signals.

In order to simulate the directional (angular) dependence of the power emitted by the GPS transmitter antenna, the 3D transmitter antenna pattern is modelled as well (L_{TX} in Eq. (1)). Since the GNSS transmitter antenna points to the Earth to serve the Earth users, this has a significant effect for space vehicles orbiting above the GPS constellation, which very often receives the GPS signal from the transmitting antenna side lobes or from the spillover around the Earth of the main lobe. Ideally, a different accurate antenna pattern corresponding to each block and signal of each constellation should be modelled. Some information about the transmitting antenna pattern of different GPS signals and blocks can be found in the literature: e.g. for the Block IIA in [17], IIR in [18] and IIF in [19]. Unfortunately, less details are available for Galileo; e.g. only the gain at boresight and at the end of the coverage of the transmitting antenna of the four Galileo IOV (In Orbit Validation) satellites is provided in [20]. In absence of more detailed information about the transmitting antenna patterns for both constellations, we used for this study the GPS transmitter antenna pattern from Block II-A (as defined in [17] and provided by Spirent [14]) to model all the transmitters for all the considered signals. Moreover, we assumed that the L1 C/A and L5Q signals are transmitted by all the GPS satellites and the E1c and E5 (E5aQ+E5bQ) signals are transmitted by all the Galileo satellites. It is therefore important to keep in mind these assumptions when evaluating our results. In particular, our

Table 1

Assumed minimum received signal power and global signal strength offset of the four considered GNSS signals.

Signal	Minimum received signal power P_{ICD} (dBm)	Global signal strength offset O_G (dB)
GPS L1 C/A	−128.5	+3
GPS L5Q	−127	+3
Galileo E1c	−130	+3
Galileo E5aQ+E5bQ	−125	+3

results should be considered as providing a qualitative indication, rather than a quantitative – even simulated – evaluation of a real behaviour.

2.3. Receiver dynamics model

The “classical” Earth–Moon *direct* transfer begins from a so called “parking orbit” around the Earth, then the orbit’s apogee is reached at the Moon’s distance or at higher altitudes by a translunar injection. To reduce the transfer time, the apogee of the translunar orbit could be chosen higher, at the expense of a slightly greater ΔV (measure of the impulse that is needed to perform a maneuver). A direct transfer typically lasts 2–5 days. Such direct transfers were used for all lunar missions from the 1960s to the 1980s, including the Luna and Apollo missions. A more novel, and less expensive, *indirect* ways of reaching the Moon exist as well, slower but cost effective [21]. However, the definition of an optimal trajectory to reach the Moon is not the goal of this study, which instead only aims to investigate the feasibility of the GNSS use for such a mission. Hence, for simplicity here we consider a direct transfer, for which the initial position and velocity of the space receiver in terms of the Keplerian orbital parameters is reported in **Table 2**. The motion of the receiver is propagated by the SimGEN software [14] from the initial condition as a function of perturbing accelerations (such as gravitational effects from the Earth, Sun and Moon, and atmospheric drag), reaching the Moon altitude after 4.5 days approximately. Half of the corresponding osculating orbit (shown in **Fig. 1**) can roughly represent an Earth–Moon Transfer Orbit (MTO). **Fig. 2** shows the first 14 h of this orbit, together with the GPS and Galileo constellation. **Fig. 3** displays the relation between time and altitude of the considered trajectory.

Table 2
Keplerian orbital parameters of the considered orbit.

Orbital Parameters	
Apogee	384,400 km
Perigee altitude	600 km
Length of the semimajor axis	195,689 km
Inclination	31
Argument of Perigee	0
Right ascension of the ascending node (RAAN)	0
True anomaly	0

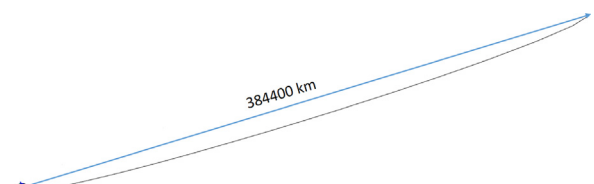


Fig. 1. Plot of half orbit defined in **Table 2**.

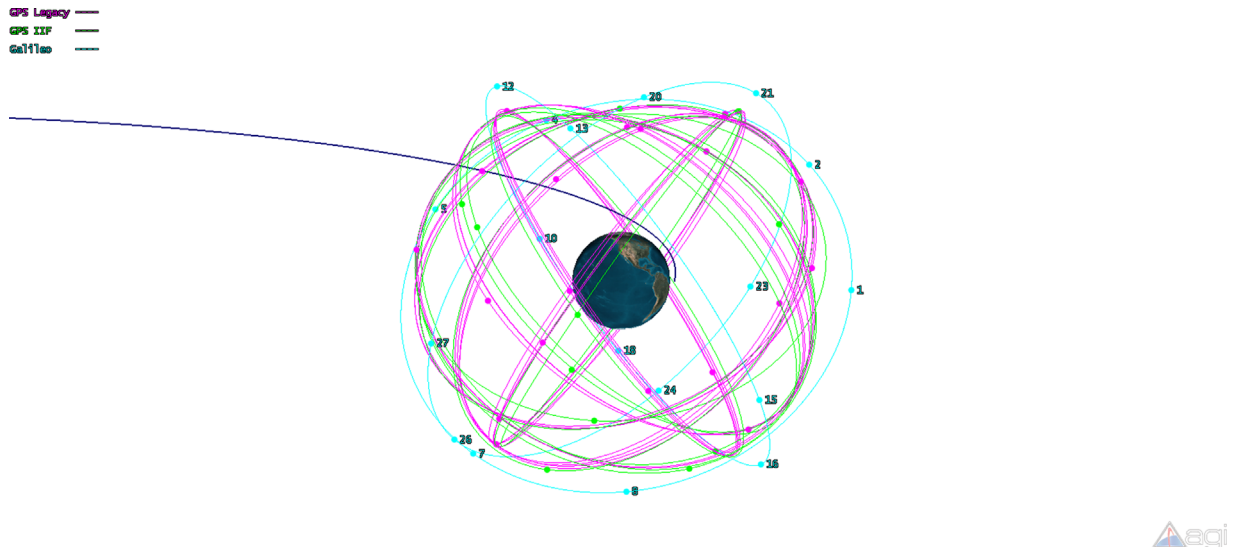


Fig. 2. Plot of the first 14 h of the defined orbit and of the GPS and Galileo constellations.

Avgi

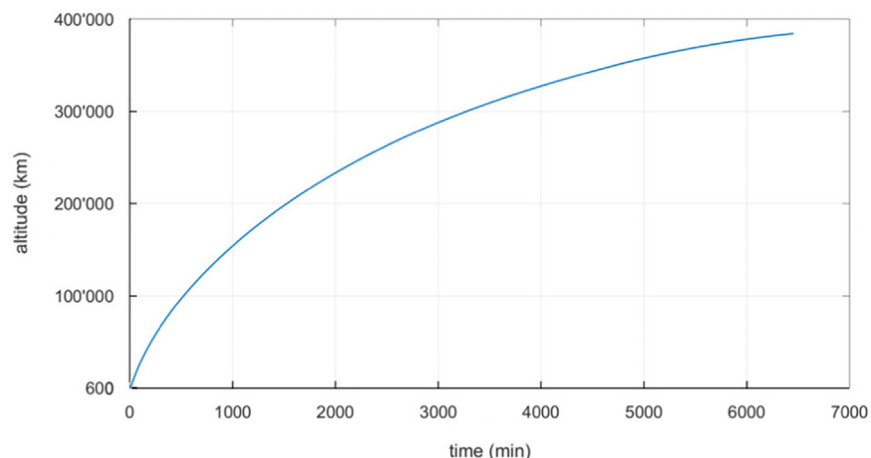


Fig. 3. Relation between time and altitude of the considered trajectory.

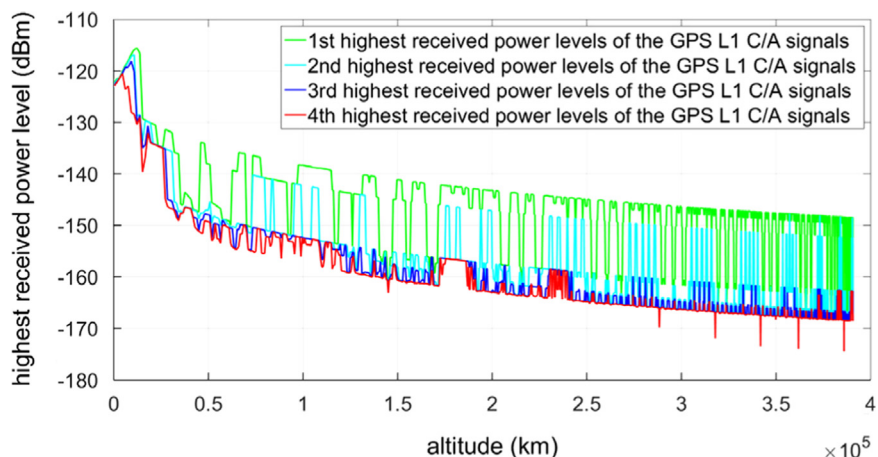


Fig. 4. First, second, third and fourth highest received power levels of the GPS L1 C/A signals as a function of the altitude, during the full considered trajectory, by assuming a 0 dBi receiver antenna gain.

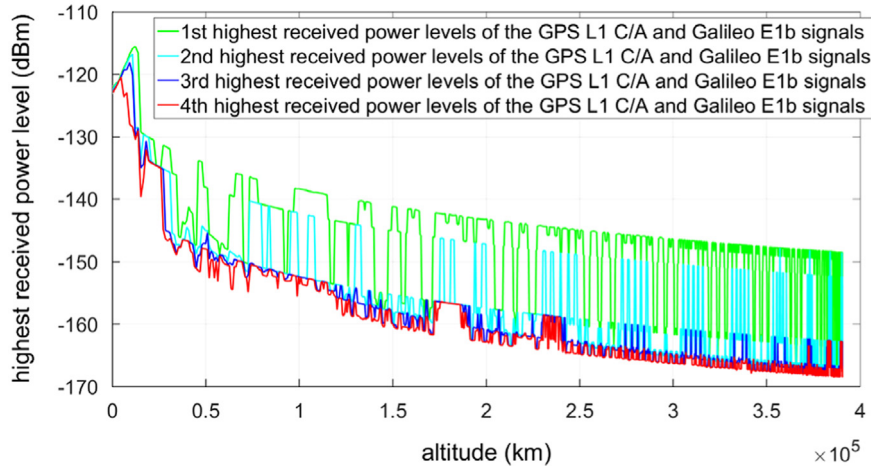


Fig. 5. First, second, third and fourth highest received power levels of the GPS L1 C/A and Galileo E1c signals as a function of the altitude, during the full considered trajectory, by assuming a 0 dBi receiver antenna gain.

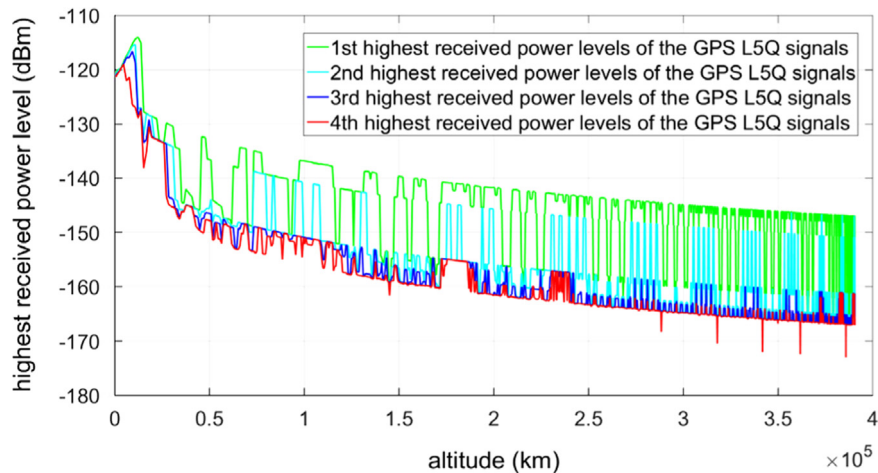


Fig. 6. First, second, third and fourth highest received power levels of the GPS L5Q signals as a function of the altitude, during the full considered trajectory, by assuming a 0 dBi receiver antenna gain.

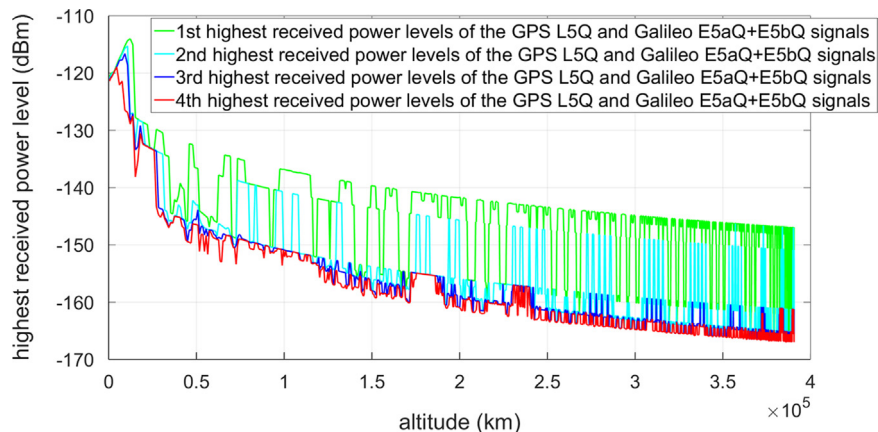


Fig. 7. First, second, third and fourth highest received power levels of the GPS L5Q and Galileo E5aQ+E5bQ signals as a function of the altitude, during the full considered trajectory, by assuming a 0 dBi receiver antenna gain.

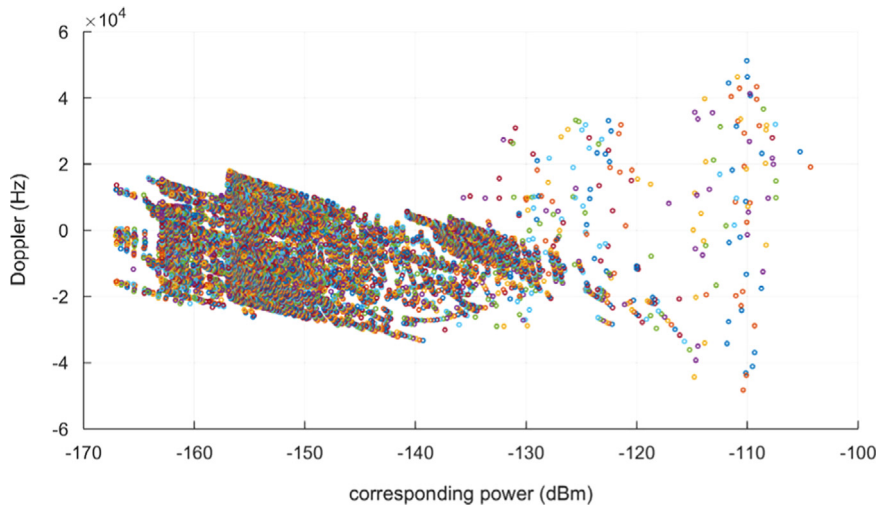


Fig. 8. Possible combinations of Doppler shift and power levels during the whole considered trajectory.

3. Signal performances

3.1. Received power levels

For the GPS L1 C/A, GPS L1 C/A–Galileo E1c combined, GPS L5Q and GPS L5Q–Galileo E5aQ+E5bQ combined constellations, respectively Figs. 4–7 show the highest received power level, the second, the third and the fourth highest received power levels, as a function of the altitude, during the full considered trajectory, by assuming a 0 dBi receiver antenna gain (L_{RX} in Eq. (1)). The fourth highest received power corresponds to a power threshold level for the receiver sensitivity, since at least four pseudoranges are required to compute the navigation solution.

3.2. Doppler shifts and Doppler rates

For the design of the acquisition of an autonomous GNSS receiver it is very useful to know the possible values of Doppler shift and Doppler rate for each received power. Figs. 8 and 9 show respectively all the possible combinations of Doppler shift-received power and all the possible combinations of Doppler rate-received power, by considering all the GPS and Galileo satellites during the full considered trajectory and by assuming a 0 dBi receiver antenna gain. As expected, the highest dynamics (Doppler shift up to 50 kHz and Doppler rate up to 65 Hz/s) are concentrated in the first portion of the trajectory (in LEO) corresponding to the highest power levels where the receiver is below the GNSS constellations. As soon as the receiver is far from the Earth (power received below –150 dBm), the Doppler is between –30 kHz and 20 kHz, and the Doppler rate is within ± 5 Hz/s.

4. Required sensitivity

As mentioned in Section 3.1, it is well known that at least four pseudoranges have to be estimated by the receiver in order to compute a GNSS standalone navigation solution. In order to estimate a pseudorange over a time

interval, the signal transmitted by the corresponding GNSS satellite has to be firstly acquired and then tracked over the same time interval.

According to the received power levels obtained by simulations and reported in Section 3.1, in this Section we identify what is the minimum power level of the four strongest signals that the receiver has to acquire and track (in order to provide the navigation solution). Such minimum power level can be considered as the required sensitivity for a receiver to provide a navigation solution. However, considering a sensitivity lower than this minimum power level may allow the receiver to measure more than four pseudoranges with a possible consequent navigation accuracy improvement.

Once that one or more sensitivity values are defined, we first specify how we assume the considered signals (GPS L1 C/A, GPS L5Q, Galileo E1c and Galileo E5aQ+E5bQ) can be processed to provide a pseudorange and secondly we verify theoretically if such sensitivity values are achievable in acquisition and tracking.

4.1. Definition of the sensitivity values

We assume a 10 dB gain for the receiving antenna; such value could be obtained during the whole trajectory by using one or more single moveable and directive (steerable) antennas on board the space vehicle, or if the size of the vehicle is big enough, by equipping it with more than one receiver antenna placed on different faces of the vehicle as in [9], in order that at least one antenna points in the GNSS satellites direction (at very high altitudes, this corresponds to an Earth-pointing space vehicle approximately).

Figs. 4–7 show that during the whole trajectory the fourth highest received power levels of respectively GPS L1 C/A, GPS L1 C/A–Galileo E1c, GPS L5Q and GPS L5Q–Galileo E5aQ+E5bQ signals do not drop below –168.5 dBm if the few peaks are neglected. This means that, by assuming a 10 dBi receiver antenna gain, a sensitivity of –158.5 dBm would allow the simultaneous

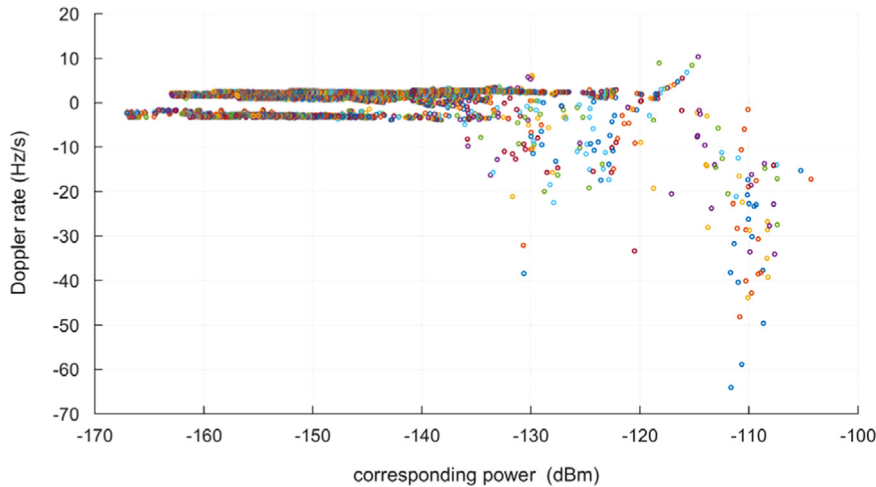


Fig. 9. Possible combinations of Doppler rate and power levels during the whole considered trajectory.

Table 3
GPS L5Q theoretical analysis (10 dB-Hz).

Desired sensitivity (dBm)	-164
Front-end noise figure (dB)	2
Sampling rate after ADC conversion (MHz)	20.46
C/N ₀ (dB-Hz)	10
Coherent integration time (s)	0.5
Coherent gain (dB)	70.10
Frequency search step (Hz)	1
Quantisation loss (dB)	-0.05
Frequency mismatch loss (dB)	-0.91
Code alignment loss (dB)	-2.50
Data bit alignment loss (dB)	0
Squaring loss (dB)	0.90
Number of non-coherent integration	19
Non-coherent gain needed (dB)	12.79
Final SNR (dB)	17.10
Total integration time needed (s)	9.5

Table 4
GPS L5Q theoretical analysis (5 dB-Hz).

Desired sensitivity (dBm)	-169
Front-end noise figure (dB)	2
Sampling rate after ADC conversion (MHz)	20.46
C/N ₀ (dB-Hz)	5
Coherent integration time (s)	1
Coherent gain (dB)	73.11
Frequency search step (Hz)	0.5
Quantisation loss (dB)	-0.05
Frequency mismatch loss (dB)	-0.92
Code alignment loss (dB)	-2.50
Data bit alignment loss (dB)	0
Squaring loss (dB)	-0.43
Number of non-coherent integration	40
Non-coherent gain needed (dB)	16.02
Final SNR (dB)	17.01
Total integration time needed (s)	40.00

detection (with a certain probability) of at least 4 GNSS satellites and the computation of a navigation solution. However, because of the poor relative geometry between the receiver and the GNSS satellites expected at very high altitudes, we have considered the three higher sensitivity values of -159, -164 and -169 dBm in order to detect (with a certain probability) a larger number of GNSS satellites (i.e., more than 4) and decrease the GDOP (as will be shown in Section 6.2).

These power values can also be expressed in terms of carrier-to-noise ratio (C/N_0). The C/N_0 is given by Eq. (2), where P_r is the received power in dBm and considering a front-end noise figure of 2 dB (assuming an effective antenna temperature of 130 K) [22]

$$C/N_0 = P_r + 174 \quad (2)$$

Using Eq. (2), the selected power thresholds of -159, -164 and -169 dBm, correspond respectively to 15, 10 and 5 dB-Hz. Next, we demonstrate that such sensitivity values can be reached by a GNSS receiver.

4.2. Theoretical analysis of acquisition and tracking sensitivities

We base our theoretical study on the wideband GPS L5Q and Galileo E5aQ+E5bQ signals, because: their power is slightly higher than the L1/E1 signals, they have a pilot channel allowing long coherent integration times, and their chipping rate is 10 times higher than the one of the L1/E1 signals (which means a much reduced tracking errors in the ranging measurements, since the ranging error is inversely proportional to the chipping rate).

According to [23], a space receiver can experience ionosphere signals delays potentially much larger (more than 150 m) than the delays on signals travelling to a receiver on the Earth (typically 2–30 m). Indeed for very high orbits, the receiver will be above the ionosphere and therefore a few signals (from the other side of the Earth) may be passing through a given altitude of the ionosphere twice. For this reason, tracking GPS L1 C/A and Galileo E1c as well as the pilot channels GPS L5Q and Galileo E5aQ+E5bQ could be desired to remove the potential high ionosphere delay. Note that once a given satellite

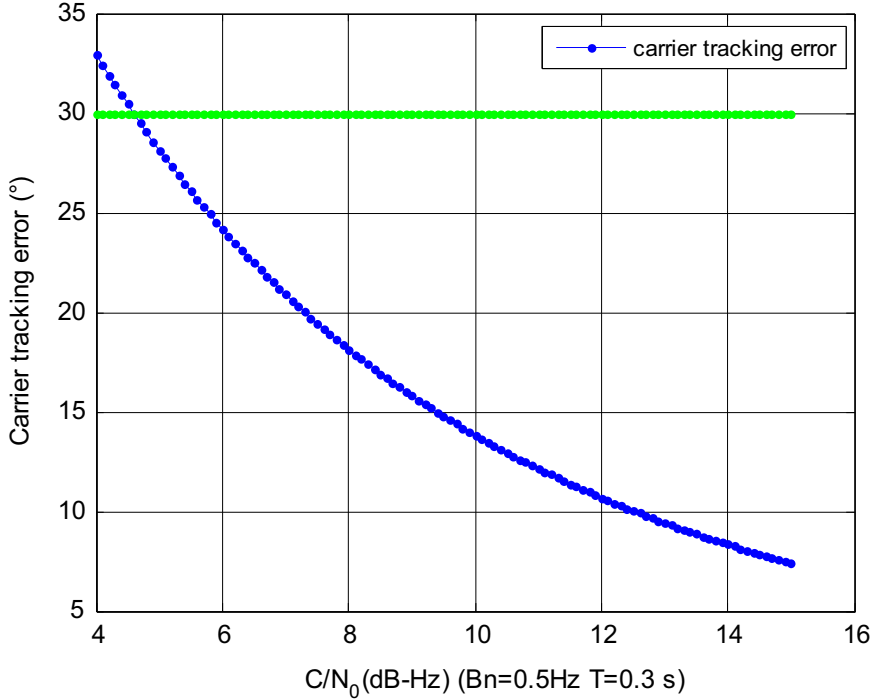


Fig. 10. Intersection between carrier tracking error and stability threshold for data-less channel.

signal frequency is tracked, it is much easier to acquire another signal frequency from the same satellite, as the code phase search can be significantly reduced [24]. Moreover, because the pilot channels and data channels in the L5 band are well synchronized with 90° carrier phase difference, it is easy to demodulate the data channel from the assistance of the L5 pilot channel. The same can be done to demodulate the data in Galileo E5aQ by using the assistance of E5aQ pilot channels.

4.3. Acquisition sensitivity and required assistance

Tables 3 and **4**, respectively report the acquisition parameters values that can be set to achieve a power sensitivity of -164 dBm (10 dB-Hz) and of -169 dBm (5 dB-Hz) (for this a final SNR of 17 dB was targeted [22], Section 6.8]), following the method proposed in [22, Chap. 6]. In both cases, the coherent integration time has been selected to decrease the squaring loss. We have selected a coherent integration time of 0.5 s for 10 dB-Hz and of 1 s for 5 dB-Hz as proposed in [25].

We note that GPS L5Q signals down to -164 dBm and -169 dBm can be acquired as reported in **Tables 3** and **4**. Therefore, Galileo E5aQ and E5bQ together can also be acquired at these power levels since their minimum received signal power is 2 dB higher (see **Table 1**).

We can also see that, since the total integration time results to be considerable (9.5 s for -164 dBm and 40 s for -169 dBm), by considering the Doppler shift values shown in **Fig. 8** and without assuming any assistance (i.e. no frequency aiding), the needed total acquisition time will be huge. Indeed, assuming that the incoming signal is stored to allow

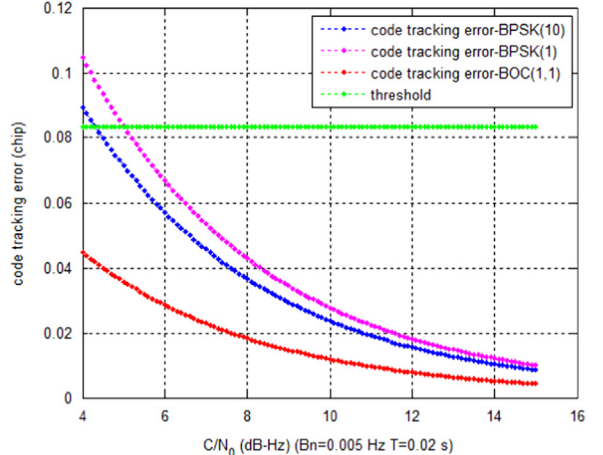


Fig. 11. Intersection between code tracking error and stability threshold.

fast processing, the total acquisition time T_A is given as

$$T_A = T_I + N_{FB} T_{FB}, \quad (3)$$

where T_I is the time required for saving the data (which corresponds to the total integration time), N_{FB} is the number of frequency bins to be searched and T_{FB} is the time needed to search one frequency bin, which is defined as

$$T_{FB} = \frac{f_S T_I}{f_{FPGA}}, \quad (4)$$

where f_S is the sampling rate, T_I is the total integration time, and f_{FPGA} is the processing frequency of the FPGA (assuming a fast Fourier transform (FFT) based correlation that computes one correlation output samples per clock cycle [26]).

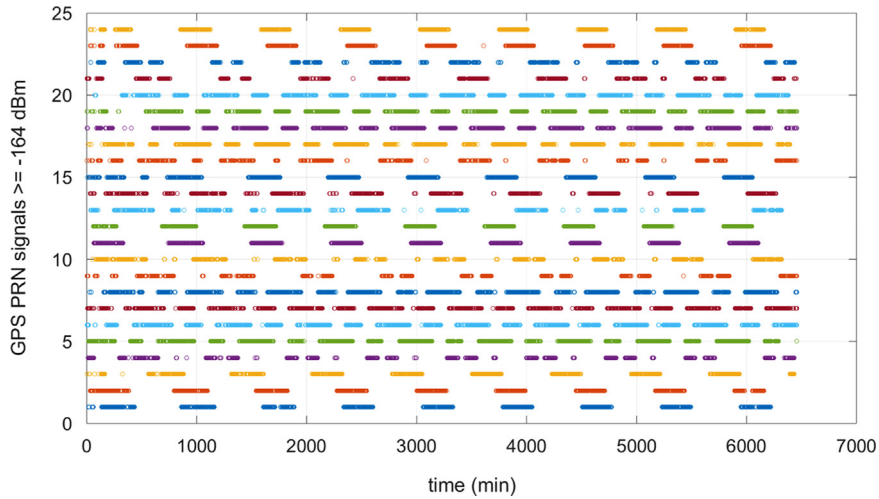


Fig. 12. Available GPS L5b signals over the time, for a sensitivity of -164 dBm (10 dB-Hz), during the whole considered trajectory.

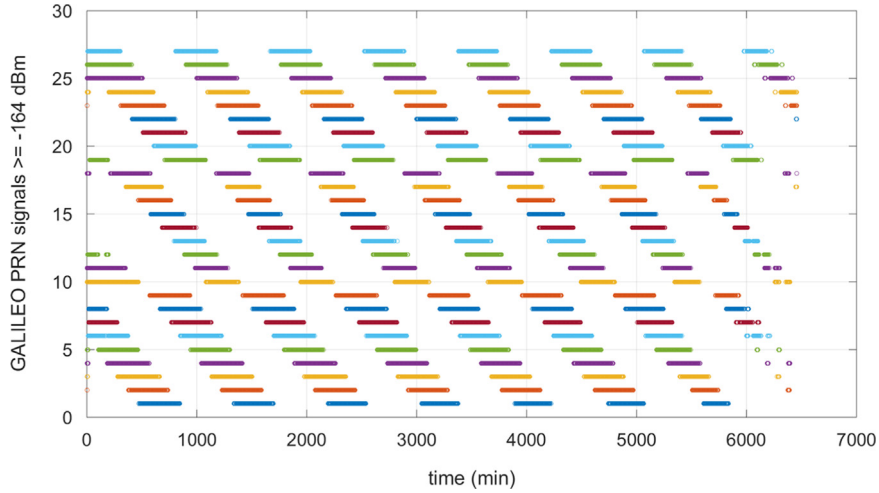


Fig. 13. Available Galileo E5aQ+E5bQ signals over the time, for a sensitivity of -164 dBm (10 dB-Hz), during the whole considered trajectory.

Table 5

Time and altitude definition of the three considered trajectory portions. The length of each portion has been set equal to 500 min, slightly higher than the duration of the longest continuous time interval of availability, which is of 475 min.

Portions definition	Portion 1	Portion 2	Portion 3
Time interval (min)	0–500	1530–2030	5960–6460
Altitude interval (km)	600–96,200	200,000–235,000	377,600–384,400

For example, for a -169 dBm sensitivity, N_{FB} is equal to 80,000 ($40,000/0.5$), and considering a 550 MHz processing clock, T_{FB} is equal to 1.488 s ($20.46 \cdot 10^6 \cdot 40/550 \cdot 10^6$). Thus, the total acquisition time needed would be 33.08 h ($40 + 1.488 \cdot 80,000/3600$). That is why the use of frequency aiding is required.

However, very precise frequency estimation with an accuracy of 0.05 Hz can be provided by an on-board orbital filter as reported in [25], or at higher rates by an orbital filter together with an inertial navigation system (INS) as considered in [27]. Furthermore, when the receiver clock offset and drift are estimated, the

frequency search space can be approximately reduced to the aiding frequency error. For a 0.05 Hz aiding accuracy, this will correspond to an acquisition time of only 41.488 s ($40 + 1.488$).

4.4. Tracking sensitivity and required assistance

The tracking process has to generate two replicas, one for the carrier and one for the code, to perfectly track and demodulate the signal of one satellite [28]. The major sources of phase error in a GNSS receiver carrier tracking loop are the phase jitter and the dynamic stress error. As

Table 6

Average GPS percentage of availability in the full trajectory duration.

Average GPS percentage of availability (dBm)	Full trajectory (%)	Portion 1 (%)	Portion 2 (%)	Portion 3 (%)
$p >= p \geq -159$	30	41	43	30
$p >= p \geq -164$	36	41	43	38
$p >= p \geq -169$	37	41	43	39

Table 7

Average Galileo percentage of availability in the full trajectory duration.

Average Galileo percentage of availability (dBm)	Full trajectory (%)	Portion 1 (%)	Portion 2 (%)	Portion 3 (%)
$p \geq -159$	16	39	21	6
$p \geq -164$	34	39	40	14
$p \geq -169$	36	39	40	40

mentioned in [12], a conservative rule of thumb for tracking threshold is that the 3-sigma jitter must not exceed one-fourth of the phase pull-in range of the PLL discriminator.

For a dataless channel (here L5Q, E5aQ or E5bQ and E1c), considering PLL four-quadrant arctangent discriminator, the pull in phase range is 360° , the 3-sigma rule threshold is therefore

$$3\sigma_{PLL} \leq 90^\circ. \quad (5)$$

This can be applied for GPS L1 C/A as well if an assistance for the data is available as proposed in [25,10].

The 1-sigma jitter σ_{PLL} can be expressed as [12]

$$\sigma_{PLL} = \sqrt{\sigma_{tPLL}^2 + \sigma_v^2 + \theta_A^2 + \frac{\theta_e}{3}} \quad (6)$$

where σ_{tPLL} is the 1-sigma thermal noise of the PLL, σ_v is the 1-sigma vibration induced oscillator jitter (here we assume a value of $\sigma_v = 1.42^\circ$ as computed in [12]), θ_A is the Allan variance induced oscillator jitter, and θ_e is the dynamic stress error.

The thermal noise of the PLL can be defined as in Eq. 5 (see [12]), where in our case $T = 0.3$ s is the tracking coherent integration time and $B_n = 0.5$ Hz is the PLL bandwidth

$$\sigma_{tPLL} = \frac{360}{2\pi} \sqrt{\frac{B_n}{C/N_0} \left(1 + \frac{1}{2TC/N_0}\right)} \quad (7)$$

If a third order loop and a high quality on-board clock is assumed (Allan deviation $\sigma_{A(r)} = 1 \times 10^{-12}$), then $\theta_A = 160(\sigma_{A(r)} f_L / Bn) = 0.504^\circ$ [12] with $f_L = 1.57542$ GHz is the Galileo E1 carrier frequency (to be conservative since E1 frequency is higher than L5, E5a and E5b frequency). Finally, from the result of our simulations, the maximum LOS jerk dynamics is $8^\circ/s^3$. Thus, $\theta_e/3 = ((d^3 R/dt^3)/3(B_n/0.7845)^3) = 10.3^\circ$, where $(d^3 R/dt^3)$ is the maximum LOS jerk dynamics. We note that such a high dynamic stress

error would be unacceptable for the tracking loop. Then a frequency aiding is required for tracking as well as for acquisition. Indeed, assuming a precise frequency assistance (as the one with 0.05 Hz accuracy reported in [25]) that can be provided by an on board orbital filter, the dynamic error θ_e will be very small. It is thus neglected in the following analysis.

The corresponding overall carrier tracking error curve, plotted as function of the C/N_0 , is shown in Fig. 10. In this figure, we also plotted the carrier tracking threshold that ensures the loop stability. We see that for 5 dB-Hz, the tracking error is below the threshold, therefore, the 5 dB-Hz sensitivity proposed for the acquisition process is also achievable for the carrier tracking.

As mentioned in [12], when there is no multipath or other distortions of the received signal and no interference, the dominant source of range error in a GPS receiver code tracking loop (DLL) is the thermal noise range error jitter and dynamic error. The rule-of thumb for tracking threshold for the DLL is that the 3-sigma value of the jitter must not exceed half of the linear pull-in range of the discriminator [12], therefore

$$3\sigma_{tDLL} = 3\sigma_{tPLL} + R_e \leq D/2, \quad (8)$$

where σ_{tDLL} is the 1-sigma thermal noise code tracking error in chip, R_e is the dynamic stress error, and D is the early-late correlator spacing in chip. Similarly as for the carrier tracking loop, because we assume precise frequency assistance, the dynamic error of the code loop is also neglected. The following formulation for the DLL thermal noise range error jitter is taken from [12], for BPSK signals (here GPS L1C/A, GPS L5Q, Galileo E5aQ and E5bQ) and valid when using a non-coherent early-late power DLL discriminator

$$\left\{ \begin{array}{l} \sigma_{tDLL} = \sqrt{\frac{B_n}{2C/N_0} D \left(1 + \frac{2}{TC/N_0(2-D)}\right)}, \quad D \geq \frac{\pi R_c}{B_{fe}} \\ \sqrt{\frac{B_n}{2C/N_0} \left[\frac{R_c}{B_{fe}} + \frac{B_{fe} T_c}{\pi - 1} \left(D - \frac{R_c}{B_{fe}}\right)^2 \right] \left(1 + \frac{2}{TC/N_0(2-D)}\right)}, \quad \frac{R_c}{B_{fe}} < D < \frac{\pi R_c}{B_{fe}} \\ \sqrt{\frac{B_n}{2C/N_0} \frac{R_c}{B_{fe}} \left(1 + \frac{1}{TC/N_0}\right)}, \quad D \leq \frac{R_c}{B_{fe}} \end{array} \right. \quad (9)$$

where $B_{fe} = 40$ MHz is the double-sided front-end bandwidth in Hz, $R_c = 1.023$ Mchip/s is the chipping rate for GPS L1 C/A and Galileo E1c while for GPS L5 and Galileo E5 this value is 10.23 Mchip/s, $D = 0.5$ is the distance between the early and late correlators in chip, $B_n = 0.005$ Hz is the code loop bandwidth in Hz, $T_c = 1/R_c$. The very small code loop bandwidth of $B_n = 0.005$ Hz is used by assuming a precise frequency assistance (as the one with 0.05 Hz accuracy reported in [25]) that can be provided by an additional on board system such as an Orbital Filter.

For a BOC(m, n) signal where pre-correlation band-limiting of the front-end can be neglected, the code tracking noise standard deviation corresponds to the one of a BPSK (n) signal multiplied by a factor $1/2\sqrt{n/m}$ (in practice this only applies to BOC(1,1) signals) [29]. Such code tracking noise standard deviation can also be approximately

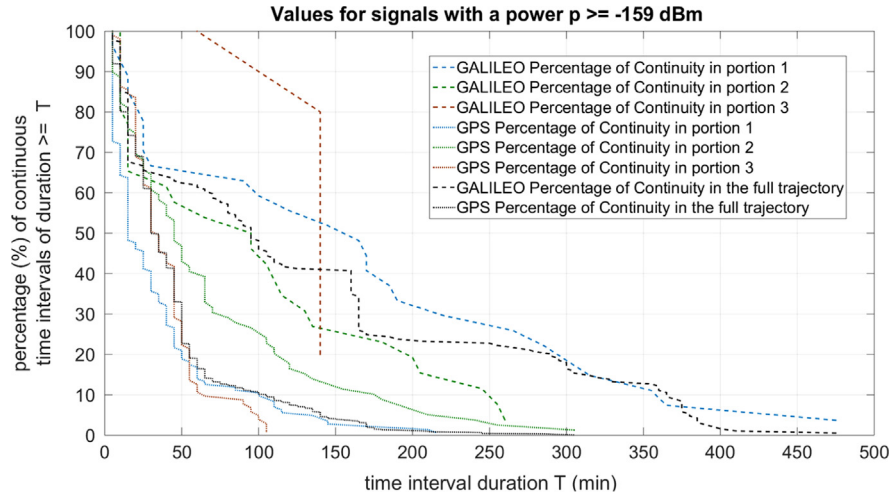


Fig. 14. Percentage of continuous time intervals (of the full trajectory or of a portion of it) that have a duration equal or longer than a time interval T for a sensitivity of -159 dBm.

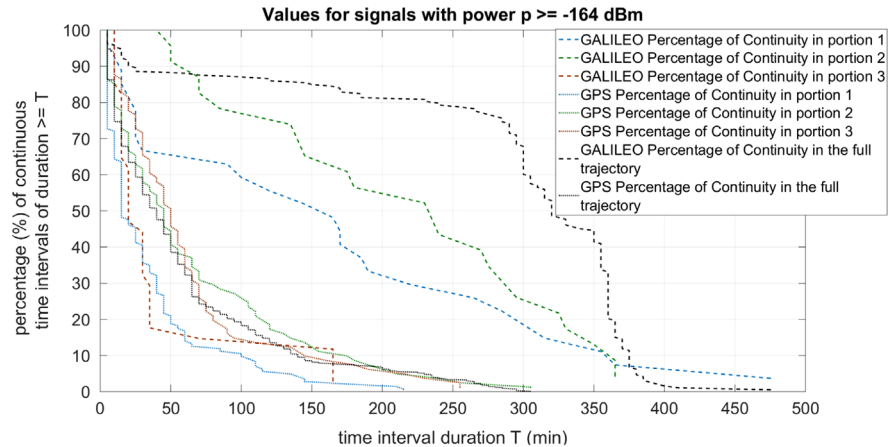


Fig. 15. Percentage of continuous time intervals (of the full trajectory or of a portion of it) that have a duration equal or longer than a time interval T for a sensitivity of -164 dBm.

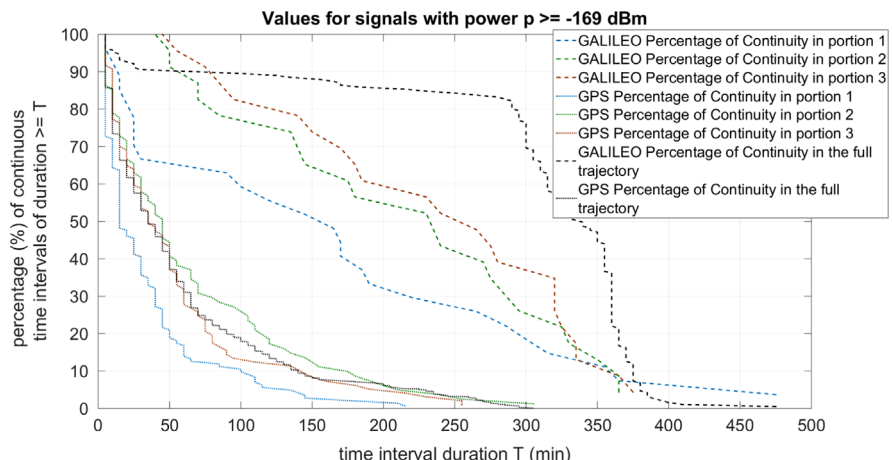


Fig. 16. Percentage of continuous time intervals (of the full trajectory or of a portion of it) that have a duration equal or longer than a time interval T for a sensitivity of -169 dBm.

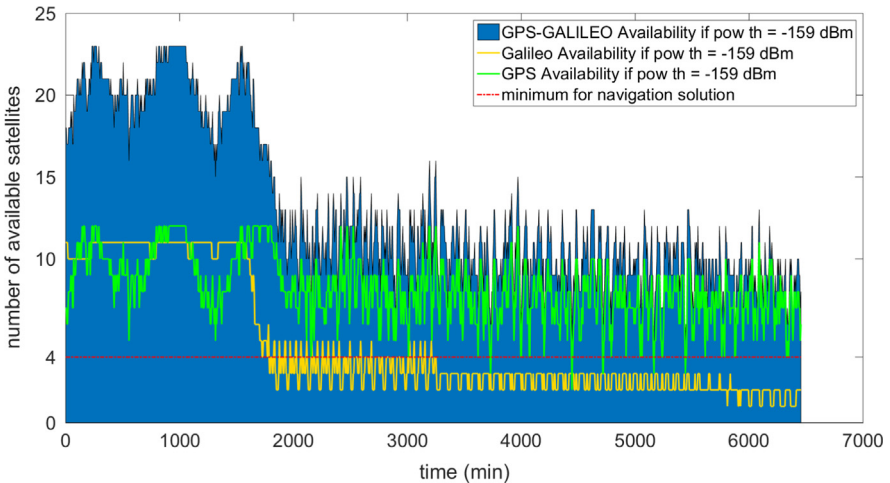


Fig. 17. Number of available satellites, for a sensitivity of -159 dBm (15 dB-Hz), during the whole considered trajectory. For Galileo the first outage of four satellites happens at time = 1795 min ($219,170$ km), then up to the time = 3260 min ($299,180$ km) there are many outages on average of 17 min with a maximum of 30 min; since time = 3260 min there are always less than 4 Galileo satellite available. Only 6 times less than 4 GPS satellites are available never more than 5 min. By considering the combined constellation there are always more than 4 satellites available.

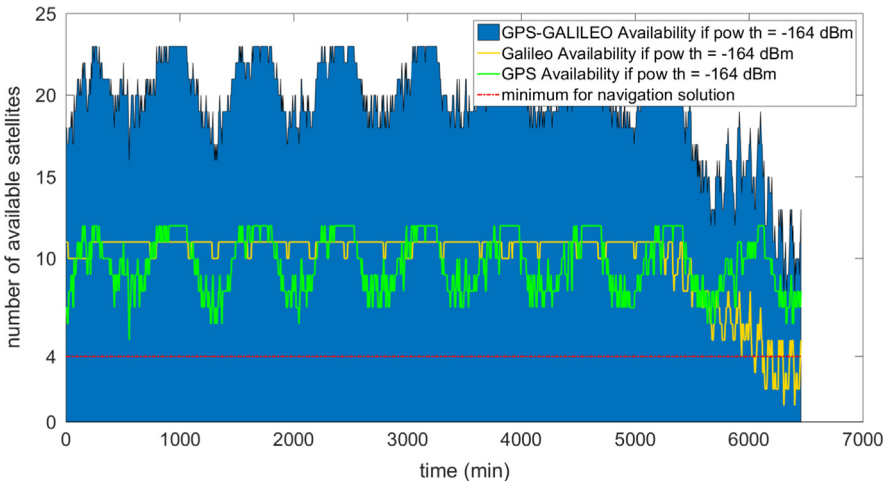


Fig. 18. Number of available satellites, for a sensitivity of -164 dBm (10 dB-Hz), during the whole considered trajectory. Only after time = 6055 min ($379,040$ km) less than 4 Galileo satellites are available for a duration within 50 min. Always more than 4 GPS satellites are available and by considering the GPS-Galileo combined constellation the minimum number of satellites simultaneously available is 8 .

assumed for Galileo E1 CBOC modulation if we only consider the BOC(1,1) component which accounts for $10/11$ of the total CBOC power (the BOC(6,1) component receives the remaining $1/11$ of the power). Therefore, for Galileo E1 this factor would be approximately $1/2\sqrt{1/2}=0.5$.

Fig. 11 shows the code tracking error for BPSK(10) (valid for Galileo E5a, E5b and GPS L5), for BPSK(1) (valid for GPS L1), and for BOC(1,1) (assumed for Galileo E1), obtained by using Eq. (9). In the same figure the tracking threshold for the DLL is plotted by using Eq. 6. The tracking threshold of the code for GPS L5 signal or Galileo E5a/E5b signal is 4.3 dB-Hz, while for L1 signal the threshold is 4.9 dB-Hz. As expected, because of the above mentioned multiplicative factor lower than 1 , for the Galileo E1 signal, the threshold is lower than for the other signals. Therefore, the 5 dB-Hz sensitivity proposed for the acquisition process is also achievable for the code tracking.

5. Resultant availability

We can define the *Availability of the GNSS signal s_i for a defined sensitivity* as a Boolean variable that is true at the time t only if

at t , the GNSS satellite from which the signal s_i is transmitted, is in the line of sight.

at t , the received power of the signal s_i is higher than the defined sensitivity.

Following the results of received power levels reported in Section 3.1 and the sensitivity values defined in Section 4, it is possible to compute the consequent *availability* of each GPS and Galileo signal along the full considered trajectory and specifically during some representative portions of it, for each

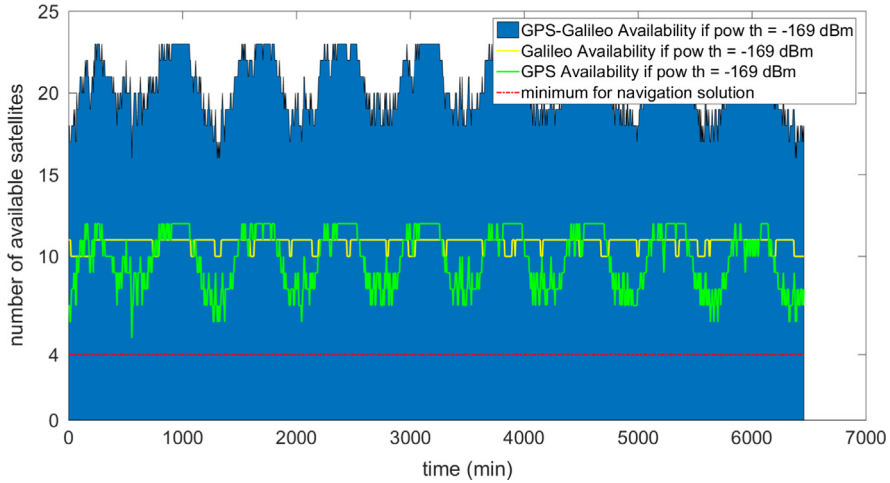


Fig. 19. Number of available satellites, for a sensitivity of -169 dBm (5 dB-Hz), during the whole considered trajectory. Respectively for a GPS, Galileo and GPS-Galileo combined constellations the minimum number of available satellites is 5, 10 and 16.

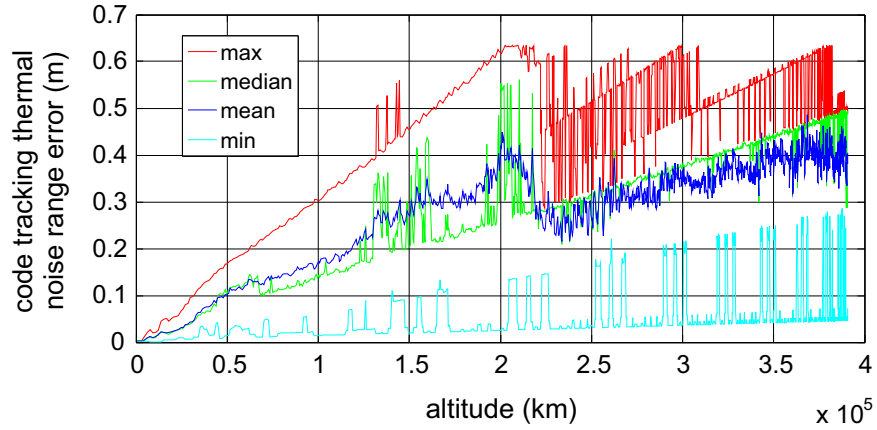


Fig. 20. BPSK(10) thermal noise code tracking error σ_{IDLL} along the altitude of the considered trajectory, for a sensitivity of -159 dBm.

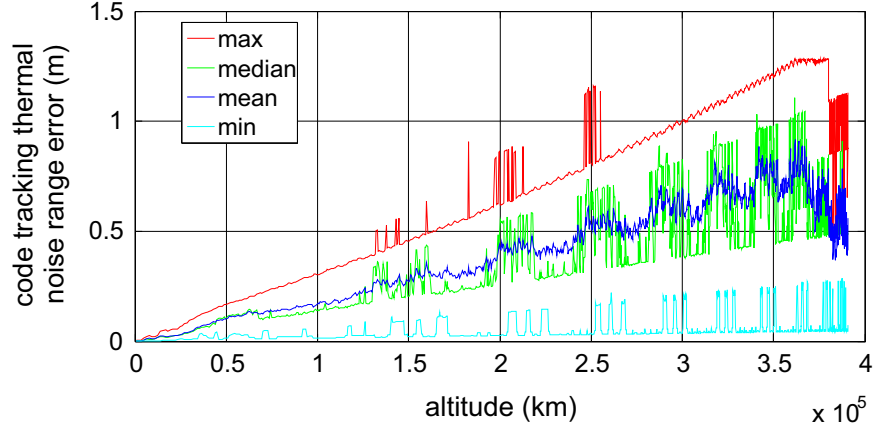


Fig. 21. BPSK(10) thermal noise code tracking error σ_{IDLL} along the altitude of the considered trajectory, for a sensitivity of -164 dBm.

of the defined sensitivity values -159 , -164 and -169 dBm. As example, Figs. 12 and 13 display the result of such computation for the sensitivity of -164 dBm, respectively for the GPS

L5b and Galileo E5aQ+E5bQ signals, along the full trajectory; for each PRN (y axis) at each instant (x axis) a point is plotted if the satellite is available. For the sensitivity of -164 dBm, the

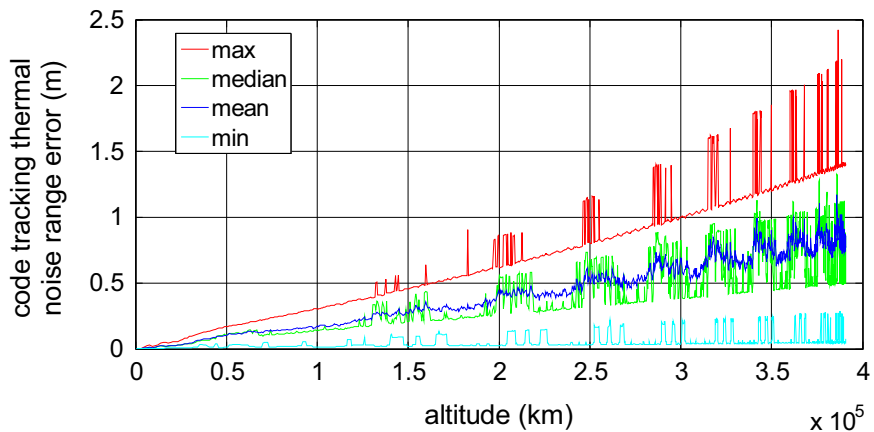


Fig. 22. BPSK(10) thermal noise code tracking error $\sigma_{t \text{ DLL}}$ along the altitude of the considered trajectory, for a sensitivity of -169 dBm .

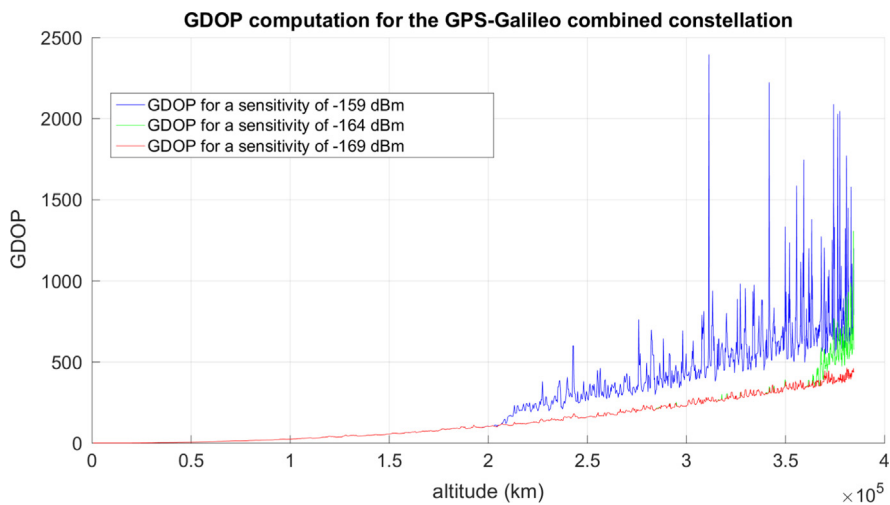


Fig. 23. GDOP values for the three considered sensitivities, for the GPS-Galileo combined constellation, for each altitude of the considered trajectory.

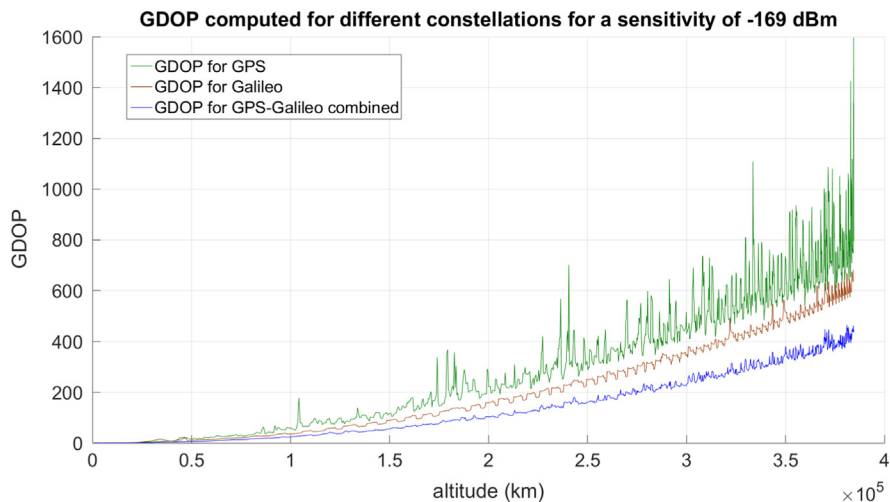


Fig. 24. GDOP value only for the -169 dBm sensitivity, for the standalone GPS, standalone Galileo and GPS-Galileo combined constellation.

average of the GPS satellites is available 40% of the full trajectory duration, while the average of the Galileo ones 34%. The same quantities are reported in [Table 6](#) for GPS and [Table 7](#) for Galileo also for the other two considered sensitivity values (-159 and -169 dBm) and for three representative portions of the trajectory defined in [Table 5](#).

Related to the availability we can also define the *Continuity of a GNSS signal s_i* as the duration of a time interval when the signal s_i is available continuously without any interruption. This is a very useful information for the acquisition module design. Since during the full trajectory or some portions of it, a signal s_i can have a number of *continuous intervals of availability* of different duration, it is useful to express the continuity in terms of *percentage of continuous time intervals (of the full trajectory or of a portion of it) that have a duration equal or longer than a time interval T* . This is shown in [Figs. 14, 15](#) and [17](#) respectively for the three defined sensitivity values, for the full trajectory and for the three defined portions, where a point of each curve identifies a time interval duration T (on the x -axis) and the corresponding percentage (on the y -axis) of continuous time intervals equal or longer than T ([Fig. 16](#)).

[Figs. 17–19](#) show the number of available satellites over time, for the GPS, Galileo and GPS-Galileo combined constellation, respectively for the three considered sensitivity values.

The obtained results show higher percentage of availability for GPS (except in portion 3 for -169 dBm) and a better continuity for Galileo. Since we assumed identic antenna patterns for the GPS and Galileo satellites (with different minimum received signal powers according the signals definitions), the different availability and continuity between the GPS and Galileo signals is certainly due to the different constellation architectures. In particular, the Galileo satellites are equally spaced in three orbital planes at the altitude of 23,222 km, while the GPS ones are distributed on six orbital at an altitude of approximately 20,200 km [[12](#)].

6. Navigation performance

6.1. Pseudorange errors

By assuming that ionosphere delays can be neglected, as mostly removable by the simultaneous reception of two frequencies from the same satellite, according to [[12](#)], at Moon altitude a significant contribution in the user equivalent range error (UERE) is the thermal noise range error jitter. In fact, it can be much higher than for terrestrial use due to the much weaker signal power levels. [Figs. 20–22](#) show the code tracking thermal range error σ_{tDL} calculated for BPSK(10) signals (valid for the considered Galileo E5aQ, Galileo E5bQ, and GPS L5), using Eq. ([9](#)), along the altitude of the considered trajectory, respectively for the three considered sensitivities. Since a different value can be computed for each signal, the maximum, median, mean and minimum of the values obtained for all the signals is displayed in the figures. It is important to underline that if the pseudorange is measured by processing the L1 band signals, due to the 10 times longer chip length, the thermal noise code tracking error would be up to ten times larger as well.

If the pseudoranges are obtained from the L5/E5 band signals with a -169 dBm sensitivity, at the Moon altitude the thermal noise code tracking error jitter σ_{tDL} reaches approximately 1 m (on average over all the signals) as shown in [Fig. 22](#). Then, neglecting atmosphere delays, by considering a multipath range error of 0.2 m, a broadcast clock error of 1.1, a broadcast ephemeris range error of 0.8 m, a receiver noise and resolution error of 0.1 m [[12](#)], at Moon altitude the user equivalent range error (UERE) would have approximately a standard deviation equal to 1.7 m ($= \sqrt{0.2^2 + 1.1^2 + 0.8^2 + 0.1^2 + 1^2}$).

6.2. Geometric dilution of precision

[Fig. 23](#) shows the GDOP values for the three considered sensitivities, for each altitude of the considered trajectory, when the GPS-Galileo double constellation is used. [Fig. 24](#) illustrates the GDOP value only for the -169 dBm sensitivity, but for the GPS-Galileo combined constellation as well as for the cases of standalone GPS and standalone Galileo constellations. The two figures clearly demonstrate the considerable benefit of the highest considered sensitivity and of the use of two GNSS constellations rather than only one. For GPS-Galileo combined constellation and a sensitivity of -169 dBm GDOP reaches the value of 400 approximately. Considering the obtained pseudorange errors for the L5/E5 band signals and the GDOP values for a sensitivity of -169 dBm, roughly the achievable accuracy (tracking L5/E5 band signals) would be within 700 m ($> 400 \cdot 1.7$ m = 680 m). However an even more accurate navigation solution can be obtained by using additional sensors and/or an orbital filter, which is anyways required to assist the acquisition and tracking of the signals as already mentioned in [Section 4.1](#).

6.3. Integration with an orbital filter

The trajectory of a space vehicles in space may be characterised by unknown, quasi-constant orbit parameters, but over the short-term it is basically identified by a finite set of parameters (the orbital parameters). The orbital parameters will change during the orbit like the MTO here considered, but the problem is still an orbit determination problem. Orbit determination consists essentially of a set of mathematical propagation techniques for predicting the future positions of an orbiting body from different kind of observations. Because of the unavoidable errors of modelling the orbital perturbations, the actual trajectory of an orbiting object tends to diverge over time (drift) from the predicted one and a new orbit determination from new observations is needed to re-calibrate knowledge of the orbit. In this case, the observations are the GNSS measurements.

As introduced in our previous work [[27](#)], for our study an Extended Kalman filter (EKF) has been implemented, which predicts the GNSS observations by propagating them through an orbital propagator and fuses them with the observations themselves. In the configuration we have implemented, pseudoranges and pseudorange rates are the inputs of the filter. The filter is adaptive, indeed the

measurement noise covariance matrix of the filter is function of the observations.

The orbital propagator used in the EKF has been implemented taking into account that during the MTO a spacecraft is influenced by a wide set of perturbations that make its orbit different from the osculating orbit. In particular, for different altitude intervals the orbital propagator relies on different sets of perturbations models. In general it includes Earth gravity (including gravity harmonics up to 6th degree and 6th order), solar radiation pressure and Sun and Moon gravity.

For our analysis, we have modelled the available pseudoranges and the pseudorange rates from the actual ranges and Doppler values provided by Spirent simulator for the scenario defined in [Section 2](#). In particular, according to [12], we have modelled the code tracking thermal range error as done in [Section 6.1](#) by using Eq. (9), a multipath range error of 0.2 m, a broadcast ephemeris range error of 0.8 m, a broadcast clock range error of 1.1 m, a receiver noise and resolution of 0.1 m. According to [12], such error components have been root-sum-squared to form the total system UERE, assumed to be Gaussian distributed.

Preliminary simulations show a position error of about 100 m (1 sigma) and a Doppler shift estimation below 0.1 Hz (1 sigma) at the Moon altitude, values very close to the ones obtained in [10,25]. The achieved accuracy results to satisfy the requirement of 100 m position accuracy for a MTO according to [10,30]. More details about models, implementation and performance of our orbital filter can be found in [31].

7. Conclusions

The reported study has investigated the potential use of a GNSS receiver for very high Earth orbits, in particular for a MTO with perigee in LEO and apogee at Moon altitude. Received power levels, Doppler shifts and Doppler rates, pseudorange errors and GDOP have been estimated and the achievable acquisition and tracking sensitivities have been briefly discussed. Using a double GNSS constellation results to be essential in order to increase the availability and also reduce the considerable GDOP. Moreover, in order to reduce the thermal noise code tracking error (very high for very weak signals) wideband signals such as the ones present in the L5/E5 band have to be used to measure the pseudoranges. In addition, a second signal from each GNSS satellite should also be processed to eliminate most of the ionosphere pseudorange error. In order to reduce the frequency bandwidth both in acquisition and in tracking, an external frequency aiding such as coming from an orbital filter is necessary. Finally the obtained results show that GNSS can be used as a navigation system for the considered trajectory with a position error below 700 m. However, according to our simulations and also to other studies, an orbital filter results can increase the position accuracy within about 100 m.

References

- [1] V. Capuano, C. Botteron, P.-A. Farine, GNSS performances for MEO, GEO and HEO, in: Proceedings of the 64th International Astronautical Congress, Beijing, China, 2013.
- [2] M.C. Moreau, P. Axelrad, J.L. Garrison, M. Wennersten, A.C. Long, Test Results of the PiVot receiver in High Earth Orbits using a GSS GPS simulator, ION, Salt Lake City, UT, 2001.
- [3] M.C. Moreau, E.P. Davis, J.R. Carpenter, D. Kelbel, G.W. Davis, P. Axelrad, Results from the GPS Flight Experiment on the High Earth Orbit AMSAT OSCAR-40 Spacecraft, ION, Portland, OR, 2002.
- [4] G. Davis, M. Moreau, R. Carpenter, F. Bauer, GPS-based navigation and orbit determination for the AMSAT AO-40 satellite, AIAA, 2003.
- [5] M.S. Braasch, M. Uijt de Haag, GNSS For, in: Proceedings of the American Astronautical Society Guidance and Control Conference, Breckenridge, CO, 2006.
- [6] W. Bamford, B. Naasz, M.C. Moreau, Navigation performance in high Earth orbits using navigator GPS receiver, in: Proceedings of the American Astronautical Society Guidance and Control Conference, Breckenridge, CO, 2006.
- [7] F.X. Marmet, E. Bondu, M. Calaprice, J. Maureau, D. Laurichesse, T. Grelier, L. Ries, GPS/Galileo navigation beyond low Earth orbit, in: Proceedings of the 6th European Workshop on GNSS Signals and Signal Processing, Neubiberg, Germany, 2013.
- [8] W.A. Bamford, G.W. Heckel, G.N. Holt, M.C. Moreau, A GPS Receiver for Lunar Missions, ION NTM, San Diego, CA, 2008.
- [9] G.B. Palmerini, M. Sabatini, G. Perrotta, En route to the Moon using GNSS signals, *Acta Astronautica* (2009).
- [10] P.F. Silva, H.D. Lopes, T.R. Peres, J.S. Silva, J. Ospina, F. Cichocki, F. Dovis, L. Musumeci, D. Serant, T. Calmettes, I. Pessina, J.V. Perelló, Weak GNSS Signal Navigation to the Moon, ION GNSS+, Nashville, TN, 2013.
- [11] [\(http://www.gps.gov/systems/gps/space/\)](http://www.gps.gov/systems/gps/space/), 2014 (last accessed on 15.07.14.)
- [12] E.D. Kaplan, C.J. Hegarty, *Understanding GPS: Principles and Applications*, Artech House, 2006.
- [13] Galileo SIS ICD Issue 1.1 September, 2010.
- [14] Spirent, Simgen Software User Manual, issue 4-02 SR02, 13th December, 2012.
- [15] ICD-GPS-200F Navstar GPS Space Segment/User Segment Interfaces, 21 September, 2011.
- [16] ICD-GPS-705C Navstar GPS Space Segment/User Segment L5 Interfaces, 5 September, 2012.
- [17] F.M. Czopek, S. Shollenberger, Description and Performance of the GPS Block I and II L-Band Antenna and Link Budget, (ION GPS1993).
- [18] A. Wu, Predictions and field measurements of the GPS block IIR L1 and L2 ground powers, in: Proceedings of the National Technical Meeting of the Institute of Navigation, San Diego, CA, 2002.
- [19] S. Erker, S. Tholert, J. Furtherth, M. Meurer, *L5 – The New GPS Signal*, 2009, IAIN, Stockholm, Schweden, 2009.
- [20] S. Arenas, F. Monjas, A. Montesano, C. Montesano, C. Mangenot, L. Salghetti, Performances of GALILEO system navigation antenna for global positioning, in: Proceedings of 5th European Conference on Antennas and Propagation, 2011.
- [21] R. Biesbroek, G. Janin, Ways to the Moon? ESA Bulletin, 103, 2000.
- [22] F. van Diggelen, *A-GPS: Assisted GPS, GNSS and SBAS*, Artech house, 2009.
- [23] R. Neville Thessin, Atmospheric Signal Delay Affecting GPS Measurements made by Space Vehicles during Launch, Orbit and Reentry, Aeronautics and Astronautics, Massachusetts Institute of Technology, 2005 (MSc. thesis).
- [24] J. Tian, Y. Wang, W. Wang, P. Shi, V. Capuano, J. Leclère, C. Botteron, P.-A. Farine, Cross-band aided acquisition on HEO orbit, in: Proceedings of the 65th International Astronautical Congress, Toronto, Canada, 2014.
- [25] L. Musumeci, F. Dovis, P.F. Silva, H.D. Lopes, J.S. Silva, Design of a very high sensitivity acquisition system for a space GNSS receiver, ION Plans, 2014.
- [26] J. Leclère, C. Botteron, P.-A. Farine, Comparison Framework of FPGA-based GNSS Signals Acquisition Architectures, *IEEE Transactions on Aerospace and Electronic Systems* 49 (3) (2013) 1497–1518.
- [27] V. Capuano, C. Botteron, Y. Wang, J. Tian, J. Leclère, P.-A. Farine, GNSS/INS/Star Tracker Integrated Navigation System for Earth-Moon Transfer Orbit, ION GNSS+, Tampa (Florida), US, 2014 September.
- [28] K. Borre, D.M. Akos, N. Bertelsen, P. Rinder, S.H. Jensen, *A Software-Defined GPS And Galileo Receiver*, Birkhäuser, 2007.
- [29] P. Groves, *Principles of GNSS, Inertial, and Multisensor Integrated Navigation Systems*, 2nd ed., Artech House, 2013.
- [30] T. Chabot, *Integrated Navigation Analysis for Moon and Mars Exploration*, Massachusetts Institute of Technology, 2005 (MSc. thesis).
- [31] F. Basile, Implementation of the orbital filter in a GNSS receiver for lunar missions, University of Rome La Sapienza, École polytechnique fédérale de Lausanne (EPFL), 2014 (MSc. thesis).